

INTERACTION OF LASER RADIATION WITH MATTER. LASER PLASMA

PACS numbers: 73.25.+i; 73.50.–h; 42.25.Ja
DOI: 10.1070/QE2015v045n07ABEH015783

Helicity-dependent photocurrent in the resistive Ag/Pd films excited by IR laser radiation

G.M. Mikheev, A.S. Saushin, V.V. Vanyukov

Abstract. **It is shown that in resistive Ag/Pd films manufactured according to the thick-film technology, in the case of oblique incidence of laser radiation of nanosecond duration at a wavelengths of 1350–2100 nm, a photon-drag photocurrent arises in the direction perpendicular to the plane of incidence, dependent on the ellipticity and sign of circular polarisation of incident radiation. This photocurrent consists of the so-called circular and linear contributions, which are, respectively, dependent on and independent of the sign of circular polarisation. In this wavelength range, the amplitude of the circular contribution is many times greater than that of the linear contribution. The results allow the use of resistive Ag/Pd films for the development and manufacture of innovative sensors of the sign of circular polarisation of pulsed laser radiation, operating in a wide spectral range.**

Keywords: *photon-drag effect, circular polarisation, sign of circular polarisation, circular photocurrent, IR radiation, resistive Ag/Pd films, sensor of the sign of circular polarisation of light.*

1. Introduction

One of interesting features of laser radiation interaction with conductive film materials is the generation of surface currents caused by different mechanisms [1–9]. Among them a special place is occupied by the circular photogalvanic effect (CPGE) [10, 11] and photon-drag effect [12, 13], which may lead to the generation of a photocurrent dependent on the degree of polarisation ellipticity and the direction of rotation of the electric field vector (the sign of circular polarisation) of the exciting light. For simplicity, this current is referred to as circular photocurrent (CPC) [14]. The studies of the CPGE are of interest from the viewpoint of the development of spintronics [15] and sensors of the sign of circular polarisation of laser radiation [14].

The CPGE arises in gyrotropic media where the symmetry with respect to mirror transformation is broken, and is conditioned by the peculiarities in the band structure of gyrotropic crystals. It was first detected in tellurium [16]. The effect was observed in the form of a photo-electromotive force generated between the end faces of a 8-mm-long cylindrical rod of crystalline tellurium, when illuminating the end-face surface by pulsed radiation from a CO_2 laser at a wavelength of 10.6 μm, directed along the geometric axis of the sample. The CPGE also manifests itself in other gyrotropic materials, for example, in bismuth silicate $Bi_{12}SiO_{20}$ [17], in quantum wells [6, 18], as well as in the crystalline films of InN at interband quantum transitions [19]. It should be noted that in quantum wells, depending on the type of symmetry, the CPGE can be observed both at oblique and normal incidence of elliptically polarised light onto the sample surface [20].

The photon-drag effect, first discovered in [21, 22], leads to the generation of the photo-electromotive force (photocurrent) by transferring the momentum of photons of incident radiation to the charge carriers in the intraband or interband energy transitions. Unlike the CPGE, the photon-drag effect can be observed in centrosymmetric media [13]. In the presence of circular polarisation of exciting radiation, the photon-drag effect can be accompanied by the CPC, which is experimentally observed at oblique incidence of a laser beam in quantum wells [23], in nanometre-thick gold films of different morphology [24, 25], in graphene under excitation in terahertz [26] and middle-IR [27] regions, and also the resistive Ag/Pd films [14, 28]. The circular photon-drag effect under excitation in the terahertz region is interpreted as the dynamic Hall effect, in which the photocurrent is caused by the Lorentz force acting on the charge carriers in electric and magnetic fields of circularly polarised exciting radiation [26].

In the case of oblique incidence of laser radiation, the transverse CPC that flows in the direction perpendicular to the plane of incidence is composed of the linear and circular contributions (see, for example, [13, 19, 26]). The linear contribution depends on the orientation of the polarisation ellipse and the degree of ellipticity of exciting radiation, and does not depend on the sign of circular polarisation, while the circular contribution depends on both these factors. Consequently, depending on the degree of radiation ellipticity, the CPC may be positive or negative with one and the same sign of circular polarisation. However, our recent study [14] has demonstrated that the ratio of the circular contribution of the transverse CPC to the linear contribution in resistive Ag/Pd films increases with increasing wavelength of exciting radiation in the spectral range of 266–1064 nm. As a result, it was found that, in a wavelength range of 529–1064 nm, the transverse CPC possesses a certain polarity for a fixed sign of circular polarisation at any degree of ellipticity. This allows employing the resistive Ag/Pd films in designing simple and high-speed sensors of the sign of circular polarisation of laser radiation.

It should be kept in mind that resistive Ag/Pd films have stable electric characteristics and have long been used in elec-

G.M. Mikheev, A.S. Saushin Institute of Mechanics, Ural Branch, Russian Academy of Sciences, ul. T. Baramzinoi 34, 426067 Izhevsk, Russia; e-mail: mikheev@udman.ru
V.V. Vanyukov Institute of Mechanics, Ural Branch, Russian Academy of Sciences, ul. T. Baramzinoi 34, 426067 Izhevsk, Russia; Institute of Photonics, University of Eastern Finland, 80101 Joensuu, Finland

Received 12 February 2015
Kvantovaya Elektronika **45** (7) 635–639 (2015)
Translated by M.A. Monastyrskiy

tronics [29]. They are widely employed in designing hybrid circuits, multichip modules and integrated microcircuit assemblies; in addition, they are used as passive electronic components such as resistors, inductance elements and multilayer capacitors [30]. It has been recently shown that resistive Ag/Pd films may be used as photovoltaic converters sensitive to the direction of the wave vector of incident radiation [31]. It is established that such converters can operate in a wide spectral range (266–1064 nm) [32].

The aim of this work is to study the CPC in resistive Ag/Pd films in a 1350–2100 nm wavelength range of exciting radiation for designing photovoltaic sensors of the sign of circular polarisation of pulsed laser radiation in a wide spectral range.

2. Preparation and main characteristics of resistive Ag/Pd films

Resistive Ag/Pd films used in our experiments were manufactured by the well-known thick-film technology [33]. A special paste containing silver oxide and palladium has been 'burned in' at the temperature of $T_{bur} = 878$ K on the dielectric surface of the substrate [31, 34]. This technique has allowed us to obtain ~20-μm-thick resistive Ag/Pd films measuring 20×20 mm on a ceramic substrate of aluminium-oxide ceramics VK-94. During the process of manufacturing, the film was equipped with two parallel film-type measuring silver electrodes mounted on the opposite sides of a square film between the substrate and the film material (Fig. 1a). The dc resistance between the electrodes closed through the film constitutes 29 Ω. Measurements have shown that the films possess p-conductivity at the concentration of charge carriers of 9.2×10^{20} cm^{-3} at their mobility of 10^{-1} cm^2 V^{-1} s^{-1}. The resistivity of the films is equal to 6.6×10^{-2} Ω cm. By means of the X-ray analysis, it has been found that the films consist of the phases AgPd, PdO and Ag_2O with a mass ratio of 80.3 : 18.7 : 1.0. The minimum sizes of crystallites of the phase components AgPd and PdO are 39 and 28 nm, respectively. Studies carried out by the scanning electron microscope (SEM) have shown that the resistive Ag/Pd films we have obtained represent a porous material (Fig. 1b). The pore size ranges from 25 to 500 nm, while the solid particles of this material have a characteristic size of 50 to 200 nm. Thus, the Ag/Pd films under investigation represent a porous structure of PdO and a solid solution of AgPd, consisting mainly of Ag [34].

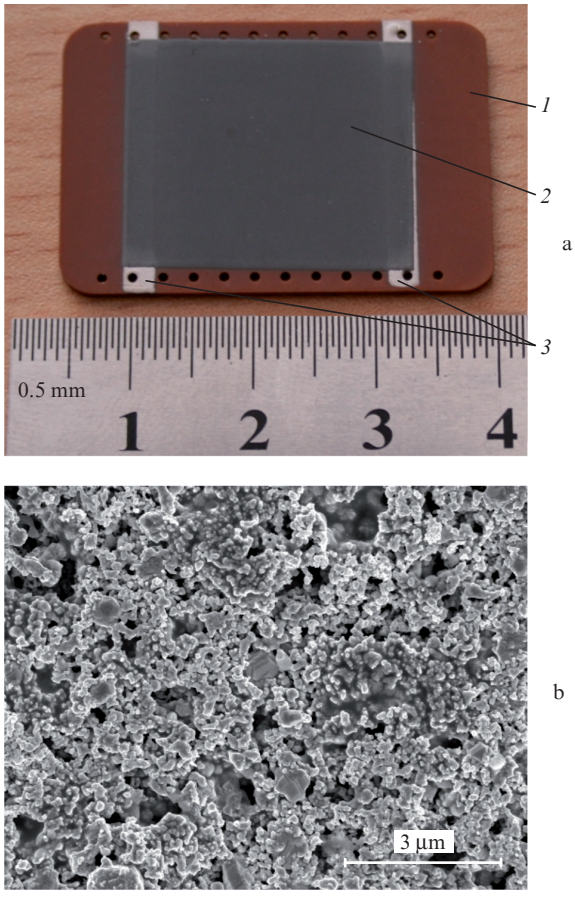

Figure 1. (a) Photograph of the Ag/Pd film and (b) SEM-image of a film surface section: (*1*) substrate; (*2*) Ag/Pd film; (*3*) silver measuring electrodes located between the substrate and film.

3. Experimental technique

In our experiments, we have used an automated frequency-tunable IR laser source (Laser Vision), consisting of an optical parametric oscillator and an amplifier based on nonlinear-optical crystals KTP and KTA. The radiation of the first and second harmonics of an electro-optically Q-switched Nd^{3+} : YAG laser operating at a pulse repetition rate of 10 Hz is used for pumping. The output wavelength of the laser source can be varied in the range of 1350–5000 nm. The pulse duration τ at the half-height is 6–8 ns depending on the wavelength, and is measured with the use of a PD-10.6-3 high-speed IR photodetector (Vigo-System Ltd) having a time constant of less than 0.2 ns and a LeCroy 42Xs digital oscilloscope with a bandwidth of 400 MHz. Averaging is performed over 100 pulses.

The pulsed radiation from the laser source having a predetermined wavelength (1350 to 2100 nm) passes through an aperture with a diameter of 4 mm, Glan polariser and an achromatic quarter-wave plate operating in the wavelength range of 900–2100 nm. Then, it falls onto the Ag/Pd film at an angle $\alpha = 45°$ (Fig. 2). At the polariser output, the laser radiation is polarised along the x' axis which lies in the vertical plane coinciding with the plane of incidence σ (p-polarised radiation). The energy E of laser pulses impinging the film is less than 3 mJ. The measuring electrodes A and B are mounted on the film in such a way that they are parallel to the plane σ (longitudinal geometry of the experiment [14]), so that the laser radiation does not fall on these electrodes during the experiment. Using a coaxial cable, the electrodes are connected directly to the input of a digital oscilloscope. The input impedance r of the oscilloscope is 50 Ω. In the experiments, we have measured the extreme value U_y of the unipolar single pulses of the photo-electromotive force, arising between electrodes A and B in the course of the film's irradiation. Herewith, the transverse CPC (i.e. the current flowing in the direction perpendicular to the incidence plane σ) can be determined by the formula $j_y = U_y/r$. Depending on experimental conditions, the values of U_y could be positive, negative, or zero.

We have experimentally studied the effect of ellipticity and sign of circular polarisation of incident radiation on the value of U_y. With this aim in view, at a fixed angle of incidence of laser radiation onto the film, $\alpha = 45°$, the value of U_y has been investigated as function of the angle of rotation γ of the quar-

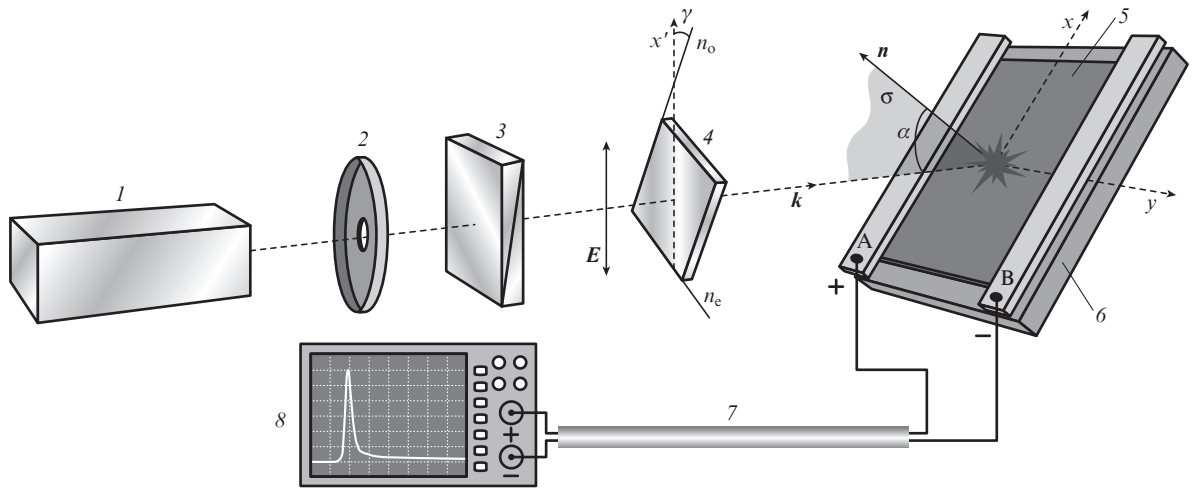

Figure 2. Schematic of the experiment: (*1*) laser light source; (*2*) diaphragm; (*3*) polariser; (*4*) achromatic quarter-wave plate; (*5*) Ag/Pd film; (*6*) substrate; (*7*) coaxial cable; (*8*) digital oscilloscope; $\boldsymbol{E}$ is the electric field vector of incident radiation; $\boldsymbol{k}$ is the wave vector; $\boldsymbol{n}$ is the normal to the film's surface; α is the angle of incidence; σ is the plane of incidence; x, y are the axes of the rectangular coordinate system ($y \perp \sigma$); A and B are the measuring electrodes positioned parallel to the plane σ; x' is the vertical axis; n_e is the optical axis of the quarter-wave plate; n_o is the axis perpendicular to the axis n_e.

ter-wave plate at different wavelengths λ, where γ is the angle between the vertical axis x' and the axis n_o perpendicular to the optical axis n_e of the plate (Fig. 2). The results are obtained by means of averaging over 100 or more laser pulses.

It is accepted that, if one looks against the direction of wave propagation, the polarisation sign is considered positive if the electric field vector rotates clockwise and negative if the rotation is counterclockwise.

4. Experimental results and discussion

Figure 3 shows typical oscillograms of the exciting laser pulses [oscillogram (*1*)] and the photovoltaic pulses arising in the film [oscillograms (*2*) and (*3*)], derived at a radiation wavelength of 2100 nm and an angle of incidence $\alpha = 45°$. Note that the photovoltaic signal is absent at $\alpha = 0$ for any parameters of incident laser radiation [14, 28, 32]. It follows from Fig. 3 that, in the case of the positive sign of circular polarisation ($\alpha = 45°$), the photovoltaic pulse has positive polarity [oscillogram (*2*)], and in the case of the negative sign ($\gamma = 135°$) – negative polarity [oscillogram (*3*)]. Thus, we observe the CPC here. Within the limits of the experiment accuracy, the leading edges of the registered photovoltaic and laser pulses coincide. However, the duration and decay time of photovoltaic pulses are much higher than those of laser pulses. The duration and decay time of laser pulses, defined in accordance with standard criteria, are equal to 7 and 6 ns, respectively, while the same parameters for photovoltaic pulses constitute in average 14 and 85 ns.

Experimental investigation of the value U_y as function of the incidence angle α show that the relation $U_y(\gamma,\alpha) = -U_y(\gamma,-\alpha)$, where $-90° < \alpha < 90°$, holds true in the entire range of wavelengths (1350–2100 nm) and for any fixed angle of γ. That means that the signal polarity depends on the direction of the wave vector $\boldsymbol{k}$ of incident radiation. According to [13, 26], this allows us to consider the observed effect as a photon-drag effect. Linear dependence of the U_y value on the incident radiation power P and its independence of the area of exposure at a fixed P [28, 32] makes it is possible to construct a dependence of the factor $\eta_y = U_y/P$ of the light power

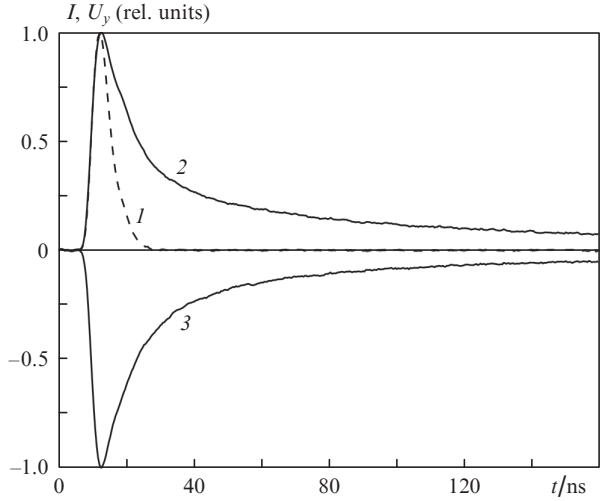

Figure 3. Oscillograms (normalised to the maximum value) of exciting laser pulse (*1*) and photo-electromotive force pulses arising at the positive (*2*) and negative (*3*) signs of circularly polarised radiation at a wavelength of 2100 nm and an incidence angle $\alpha = 45°$.

conversion into the pulsed voltage U_y on the rotation angle γ at a fixed wavelength λ. As an example, Fig. 4 demonstrates the normalised experimental dependence $\bar{\eta}_y(\gamma) = \eta_y(\gamma)/\eta_y^{max}$ obtained for $\lambda = 1750$ nm, where η_y^{max} is the maximum absolute value of η_y in the range $0 \leqslant \gamma \leqslant 180°$. It can be seen that the signal is absent at $\gamma = 0$, 90°, 180° (p-polarised light). Photo-electromotive force is also absent in the case of s polarisation, which has been proven by additional experiments. The signal in Fig. 4 is positive for circular polarisation with the positive sign ($0 < \gamma < 90°$) and negative for circular polarisation with the negative sign ($90° < \gamma < 180°$), the conversion factor $\bar{\eta}_y(\gamma)$ depending considerably on the degree of ellipticity of light polarisation, i.e. on the angle γ. The resultant normalised experimental dependence can be well approximated by the function [Fig. 4, curve (*1*)]:

$$\bar{\eta}_y = \eta_{02}\sin 2\gamma - \eta_{04}\sin 4\gamma, \qquad (1)$$

where $\eta_{02} = 0.986$ and $\eta_{04} = 0.083$ are the amplitudes of the circular and linear contributions, respectively ($\xi = \eta_{02}/\eta_{04} = 11.9$). Curves (*2*) and (*3*) in Fig. 4 describe circular ($\eta_{02}\sin 2\gamma$) and linear ($-\eta_{04}\sin 4\gamma$) contributions, which are, respectively, dependent on and independent of the sign of circular polarisation. It can be seen that, at angles $0 < \gamma < 90°$, the circular contribution is positive, while the linear contribution changes the polarity, and, in addition, the relation $\eta_{02} \gg \eta_{04}$ holds true.

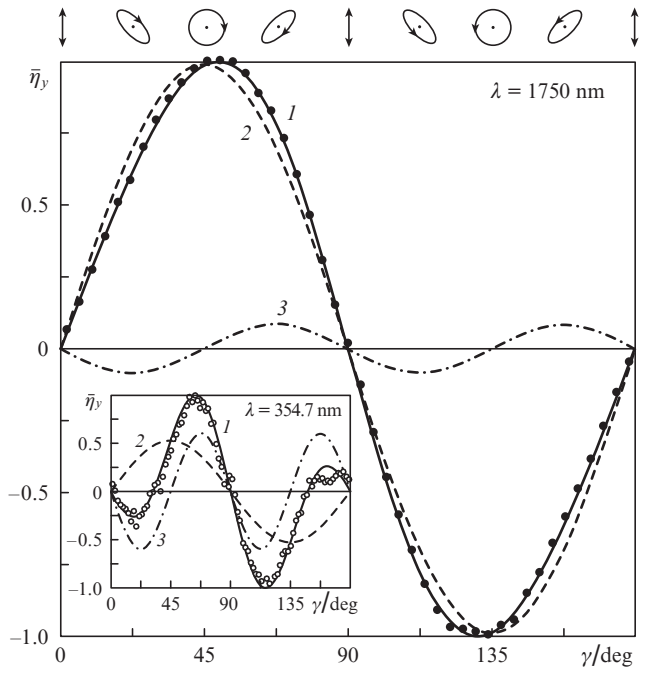

Figure 4. Dependences of the normalised factor of the laser power conversion into the photo-electromotive force on the angle γ (dots), obtained for the excitation wavelengths of 1750 and 354.7 nm [14] (insert). Curves (*1*) show approximating dependences, curves (*2*) and (*3*) – dependences of circular and linear contributions, respectively. Polarisation ellipses of radiation for different angles γ are shown at the top.

Similar experimental dependences of $\bar{\eta}_y(\gamma)$ have been obtained for the wavelengths of 1350, 1450, 1650, 1850, 1950 and 2100 nm. As a result of their mathematical processing with regard to the data of paper [14], the dependence $\xi(\lambda)$ has been plotted (Fig. 5). It is seen that, in the UV spectral region, the ratio $\xi = \eta_{02}/\eta_{04}$ is comparable with unity, whilst in the IR region for the wavelengths of 1350–2100 nm the amplitude η_{02} of the circular contribution is many times greater than the amplitude η_{04} of the linear contribution. Thus, it may be assumed that virtually 'pure' circular photon-drag effect is observed in the wavelength range of 1350–2100 nm.

Expression (1) indicates that, for the clockwise-polarised light ($0 < \gamma < 90°$), the normalised conversion factor $\bar{\eta}_y$ is positive for $\xi > 2$. As a result of linear approximation of the first four points in the shortwave spectral region shown in Fig. 5, it was found that the condition $\xi > 2$ is fulfilled for $\lambda >$ 529 nm. This means that in the spectral range $529 < \lambda \leqslant$ 2100 nm, for above-represented experimental geometry and electrical circuitry connecting the measuring electrodes to oscilloscope, the photovoltaic signal has positive polarity in the case of the positive sign of circular polarisation and negative polarity in the case of the negative sign. However, for λ

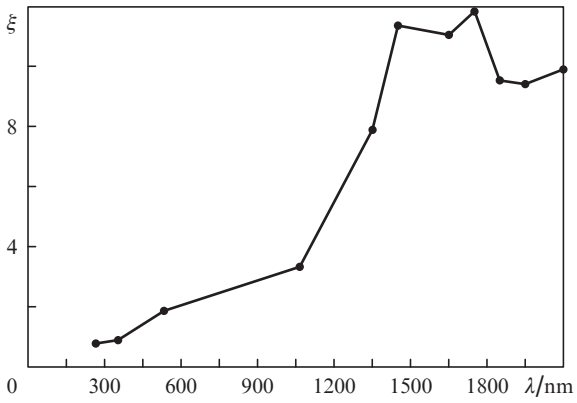

Figure 5. Ratio ξ of the amplitudes of circular and linear contributions for the transverse CPC vs. the incident radiation wavelength λ.

<529 nm, depending on the ellipticity degree γ, the conversion factor $\bar{\eta}_y$ can take both positive and negative values for one and the same sign of circular polarisation of light. This fact is well demonstrated by the dependence $\bar{\eta}_y(\gamma)$ obtained in [14] for $\lambda = 354.7$ nm (see the inset in Fig. 4), for which $\eta_{02} = 0.53$, $\eta_{04} = 0.6$, whilst the value ξ turns out less than unity and constitutes 0.88.

The photocurrent due to the photon-drag effect, with linear and circular polarisations of exciting radiation, has also been investigated in porous nanographite films [35, 36], and the films of single-walled nanotubes [9, 37] in the visible and infrared regions. However, the CPC is not observed in these nanocarbon films. Meanwhile, as the results obtained clearly demonstrate, the CPC is observed in the resistive Ag/Pd films in a wide spectral range. Why it is so and what properties of the Ag/Pd films are responsible for the CPC generation in the photon-drag effect remain unexplained and present the subject of further research. Nevertheless, it is clear that it is already possible to create sensors of the sign of circular polarisation of pulsed laser radiation on the basis of resistive Ag/Pd films.

Thus, in porous resistive Ag/Pd films consisting of PdO and AgPd, in the framework of experimental geometry with the measuring electrodes being parallel to the plane of incidence of exciting radiation, the circular photon-drag effect is observed within a wide range of radiation wavelengths (266–2100 nm), which leads to generation of the photovoltaic current dependent on the ellipticity and sign of circular polarisation. In the wavelength range of 529–2100 nm, the polarity of the photocurrent (photo-electromotive force) is unambiguously determined by the sign of circular polarisation. These results demonstrate the possibility of employing resistive Ag/Pd films for the development and creation of high-performance sensors which allow us, by possessing the information on the polarity of a single registered photovoltaic pulse, to determine the sign of circular polarisation of the incident light pulse in a wide range of wavelengths.

Acknowledgements. The authors thank Yu.P. Svirko from the University of Eastern Finland, as well as V.M. Styapshin from the Institute of Mechanics, Ural Branch of the Russian Academy of Sciences, for discussions of the results obtained.

This work was supported by the Russian Foundation for Basic Research (Grant No. 13-08-01031) and the Finnish Academy of Sciences (Grant No. 288547).

References

1. Von Gutfeld R.J. *Appl. Phys. Lett.*, **23** (4), 206 (1973).
2. Konov V.I., Nikitin P.I., Satyukov D.G., et al. *Izv. Akad. Nauk SSSR. Ser. Fiz.*, **55**, 1343 (1991).
3. Nikishkin V.A., Sevenyuk A.A., Sukhov A.V. *Kvantovaya Elektron*., **18** (9), 1103 (1991) [*Sov. J. Quantum Electron*., **21** (9), 999 (1991)].
4. Beregulin E.V., Pavlov P.M., Rivkin S.M., et. al. *Pis'ma Zh. Eksp. Teor. Fiz.*, **25** (2), 113 (1977).
5. Mikheev G.M., Zonov R.G., Obraztsov A.N., et. al. *Pis'ma Zh. Tekh. Fiz.*, **31** (3), 11 (2005).
6. Ganichev S.D., Prettl W. *J. Phys. Condens. Matter.*, **15**, 935 (2003).
7. Vengurlekar A.S., Ishihara T. *Appl. Phys. Lett.*, **87** (9), 091118 (2005).
8. Noginova N., Yakim A.V., Soimo J., et al. *Phys. Rev. B*, **84** (3), 035447 (2011).
9. Mikheev G.M., Nasibulin A.G., Zonov R.G., et al. *Nano Lett.*, **12** (1), 77 (2012).
10. Asnin V.M., Bakun A.A., Danishevskii A.M., et al. *Solid State Commun.*, **30**, 565 (1979).
11. Belinicher V.I., Sturman B.I. *Usp. Fiz. Nauk*, **130** (3), 415 (1980).
12. Belinicher V.I. *Fiz. Tverd. Tela*, **23**, 461 (1981).
13. Glazov M.M., Ganichev S.D. *Phys. Rep.*, **535** (3), 101 (2014).
14. Mikheev G.M., Saushin A.S., Zonov R.G., Styapshin V.M. *Pis'ma Zh. Tekh. Fiz*, **40** (10), 37 (2014).
15. Kusraev J.G. *Usp. Fiz. Nauk*, **180** (7), 759 (2010).
16. Asnin V.M., Bakun A.A., Danishevskii A.M., et. al. *Pis'ma Zh. Eksp. Teor. Fiz.*, **28** (2), 80 (1978).
17. Petrov M.P., Grachev A.I. *Pis'ma Zh. Eksp. Teor. Fiz*., **30** (1), 18 (1979).
18. Yu J., Chen Y., Cheng S., Lai Y. *Physica E: Low Dimens. Syst. Nanostruct.*, **49**, 92 (2013).
19. Zhang Z., Zhang R., Liu B., et al. *Solid State Commun.*, **145** (4), 159 (2008).
20. Ivchenko E.L. *Usp. Fiz. Nauk*, **172** (12), 1461 (2002).
21. Danishevskii A.M., Kastal'skii AA, Rivkin S.M., Yaroshetskii I.D. *Zh. Eksp. Teor. Fiz.*, **58** (2), 544 (1970).
22. Gibson A.F., Kimmitt M.F., Walker A.C. *Appl. Phys. Lett.*, **17** (2), 75 (1970).
23. Shalygin V.A., Diehl H., Hoffmann C., et al. *Pis'ma Zh. Eksp. Teor. Fiz.*, **84** (10), 666 (2006).
24. Hatano T., Ishihara T., Tikhodeev S., Gippius N. *Phys. Rev. Lett.*, **103** (10), 103906 (2009).
25. Akbari M., Onoda M., Ishihara T. *Opt. Express.*, **23** (2), 823 (2015).
26. Karch J., Olbrich P., Schmalzbauer M., et al. *Phys. Rev. Lett.*, **105** (22), 227402 (2010).
27. Jiang C., Shalygin V.A., Panevin V.Y., et al. *Phys. Rev. B*, **84**, 125429 (2011).
28. Mikheev G.M., Aleksandrov V.A., Saushin. *Pis'ma Zh. Tekh. Fiz.*, **37** (12), 16 (2011).
29. Melan E.H. *Microelectron. Reliab.*, **6**, 53 (1967).
30. Wang S.F., Dougherty J.P., Huebner W., Pepin J.G. *J. Am. Ceram. Soc.*, **77** (12), 3051 (1994).
31. Mikheev G.M., Zonov R.G., Aleksandrov V.A., Russkikh L.M. Russian Patent No. 2365027 (2009).
32. Mikheev G.M., Zonov R.G., Aleksandrov V.A. *Pis'ma Zh. Tekh. Fiz.*, **36** (14), 79 (2010).
33. Larry J.R., Rosenberg R.M., Uhler R.O. *IEEE Trans. Compon., Hybrids, Manuf. Technol.*, **3** (2), 211 (1980).
34. Mikheev G.M., Saushin A.S., Goncharov O.Yu., et al. *Fiz. Tverd. Tela*, **56** (11) 2212 (2014).
35. Mikheev G.M., Styapshin V.M., Obraztsov P.A., et al. *Kvantovaya Elektron*., **40** (5), 425 (2010) [*Quantum Electron*., **40** (5), 425 (2010)].
36. Obraztsov P.A., Mikheev G.M., Garnov S.V., et al. *Appl. Phys. Lett.*, **98** (9), 091903 (2011).
37. Saushin A.S., Zonov R.G., Nasibulin A.G., Mikheev G.M. *Proc. NPO'4 Fourth Int. Work. Nanocarbon Photonics Optoelectron* (Finland, University of Eastern Finland, 2014).